Research Article | Vol. 9, No. 8 | 1 Aug 2018 | BIOMEDICAL OPTICS EXPRESS 3503
Biomedical Optics EXPRESS

Hyperspectral imaging in highly scattering media by the spectral phasor approach using two filters

ALEXANDER DVORNIKOV AND ENRICO GRATTON*

Laboratory for Fluorescence Dynamics, Department of Biomedical Engineering, University of California Irvine, Irvine, CA 92697, USA
**egratton22@gmail.com*

Abstract: Hyperspectral imaging is a common technique in fluorescence microscopy to obtain the emission spectrum at each pixel of an image. However, methods to obtain spectral resolution based on diffraction gratings or integrated prisms work poorly when the sample is strongly scattering. We developed a microscope named the DIVER that collects the fluorescence emission over a very large angle. Since the fluorescence light after passing through the multiple scattering sample is not collimated, the use of grating or prisms strongly limits the amount of light that can be used with available hyperspectral devices. Here we show that 2 filters that accept uncollimated light over a large aperture are sufficient to calculate the spectral phasor rather than displaying the entire spectrum. Using the properties of the spectral phasors, we can resolve spectral components and perform the type of data analyses that are usually performed in hyperspectral image analysis.

OCIS codes: (110.0110) Imaging systems; (180.0180) Microscopy.

References and links

1. L. M. Andrews, M. R. Jones, M. A. Digman, and E. Gratton, "Detecting Pyronin Y labeled RNA transcripts in live cell microenvironments by phasor-FLIM analysis," Methods Appl. Fluoresc. **1**(1), 015001 (2013).
2. F. Cutrale, A. Salih, and E. Gratton, "Spectral Phasor approach for fingerprinting of photo-activatable fluorescent proteins Dronpa, Kaede and KikGR," Methods Appl. Fluoresc. **1**(3), 035001 (2013).
3. L. Malacrida, S. Astrada, A. Briva, M. Bollati-Fogolín, E. Gratton, and L. A. Bagatolli, "Spectral phasor analysis of LAURDAN fluorescence in live A549 lung cells to study the hydration and time evolution of intracellular lamellar body-like structures," Biochim. Biophys. Acta **1858**(11), 2625–2635 (2016).
4. L. Malacrida, E. Gratton, and D. M. Jameson, "Model-free methods to study membrane environmental probes: a comparison of the spectral phasor and generalized polarization approaches," Methods Appl. Fluoresc. **3**(4), 047001 (2015).
5. L. Malacrida, D. M. Jameson, and E. Gratton, "A multidimensional phasor approach reveals LAURDAN photophysics in NIH-3T3 cell membranes," Sci. Rep. **7**(1), 9215 (2017).
6. S. Ranjit, A. Dvornikov, M. Levi, S. Furgeson, and E. Gratton, "Characterizing fibrosis in UUO mice model using multiparametric analysis of phasor distribution from FLIM images," Biomed. Opt. Express **7**(9), 3519–3530 (2016).
7. F. Fereidouni, A. N. Bader, A. Colonna, and H. C. Gerritsen, "Phasor analysis of multiphoton spectral images distinguishes autofluorescence components of in vivo human skin," J. Biophotonics **7**(8), 589–596 (2014).
8. F. Fereidouni, A. N. Bader, and H. C. Gerritsen, "Spectral phasor analysis allows rapid and reliable unmixing of fluorescence microscopy spectral images," Opt. Express **20**(12), 12729–12741 (2012).
9. P. Wang, G. Turcatel, C. Arnesano, D. Warburton, S. E. Fraser, and F. Cutrale, "Fiber pattern removal and image reconstruction method for snapshot mosaic hyperspectral endoscopic images," Biomed. Opt. Express **9**(2), 780–790 (2018).
10. F. Cutrale, V. Trivedi, L. A. Trinh, C. L. Chiu, J. M. Choi, M. S. Artiga, and S. E. Fraser, "Hyperspectral phasor analysis enables multiplexed 5D in vivo imaging," Nat. Methods **14**(2), 149–152 (2017).
11. Z. Lavagnino, J. Dwight, A. Ustione, T. U. Nguyen, T. S. Tkaczyk, and D. W. Piston, "Snapshot Hyperspectral Light-Sheet Imaging of Signal Transduction in Live Pancreatic Islets," Biophys. J. **111**(2), 409–417 (2016).
12. A. D. Elliott, L. Gao, A. Ustione, N. Bedard, R. Kester, D. W. Piston, and T. S. Tkaczyk, "Real-time hyperspectral fluorescence imaging of pancreatic β-cell dynamics with the image mapping spectrometer," J. Cell Sci. **125**(20), 4833–4840 (2012).
13. V. Crosignani, A. S. Dvornikov, and E. Gratton, "Enhancement of imaging depth in turbid media using a wide area detector," J. Biophotonics **4**(9), 592–599 (2011).

#329008 https://doi.org/10.1364/BOE.9.003503
Journal © 2018 Received 23 Apr 2018; revised 14 Jun 2018; accepted 18 Jun 2018; published 3 Jul 2018

Biomedical Optics EXPRESS

14. L. Malacrida, E. Gratton, and D. M. Jameson, "Model-free methods to study membrane environmental probes: a comparison of the spectral phasor and generalized polarization approaches," Methods Appl. Fluoresc. **3**(4), 047001 (2015).

1. Introduction

Spectral phasors were recently introduced as an alternative to spectral demixing, for the determination of FRET and for the measurement of dipolar relaxation of probes in membranes [1–8]. The basic concept in the spectral phasor approach is that the entire spectrum is not needed for some of the classical spectral analysis techniques such as demixing, but only few parameters of the spectral distribution are sufficient for these calculations. In the original papers in this area [1,2] the focus was on using the zero and first component of the spectral Fourier transform as a proxy for the entire spectrum. In the case in which the spectrum is dominated by few spectral bands, this approach is very efficient and provides fast and valid alternatives to the analysis of the full spectrum. This is particularly convenient in cases like spectral analysis during surgery, in live animals studies [9,10] and in all those cases in which full hyperspectral imaging is not feasible or inconvenient.

One example of a system that could greatly benefit from the phasor analysis approach in tissue spectroscopy (absorption and fluorescence) is the case in which the light to be collected has undergone multiple scattering. The multiple-scattered light travels in all directions so that it cannot be easily focused on the entrance slit of a dispersive element or transformed in a parallel beam for use with hyperspectral cameras. In thick-tissue spectroscopy, the light, after being transmitted through the tissue, is emitted over a very large cone angle. The various schemes available to capture this transmitted (or fluorescence) light only use a relatively narrow angle of the emitted light with severe reduction of the signal [11,12].

We introduced in 2011 a microscope design (called the DIVER) that can capture a very large solid angle of the emitted light (close to 2π) and we have shown that this microscope, depending on the tissue thickness, can capture several orders of magnitude more light than conventional microscopes [13]. An advantage (and limitation) of the DIVER design is that the transmitted fluorescence is not collimated. Therefore, in the transmitted path of the DIVER microscope, glass filters are employed since these filters are largely insensitive to the incident angle, which could be very large. We show here that plastic filters that can be used for this purpose are available (Cyan and Green filters from Neewer 18x20cm Transparent Color Correction Lighting Gel Filter Set, available for $10.99 on Amazon cat# B016Q0BA6A) and we describe their use in the DIVER microscope to obtain hyperspectral information using the spectral phasor approach.

2. Classical calculation of the spectral phasor components

In the common application of the spectral phasor method [4,13], the transmitted or fluorescence emission is collected with a spectrograph to provide the spectrum that we indicate by $I(\lambda)$ over a spectral band $\Delta\lambda$.

We define the G and S components of the spectral phasor to be [14]

$$G = \sum_\lambda I(\lambda) * cos(n * 2\pi * \lambda / \Delta\lambda) / \sum_\lambda I(\lambda) \quad (1)$$

$$S = \sum_\lambda I(\lambda) * sin(n * 2\pi * \lambda / \Delta\lambda) / \sum_\lambda I(\lambda) \quad (2)$$

where the sum is calculated in the bandwidth $\Delta\lambda$ and n is an index to characterize the harmonics in the Fourier coefficients given by the G and S expressions. The G and S components obtained using this calculation are plotted in a polar plot called the spectral phasor plot for every pixel of an image or for different locations in a tissue sample [14].

For multiple scattering samples, the collection of $I(\lambda)$ can be problematic. Let us consider first the case of collection of the fluorescence from a scattering sample. We assume that the direct excitation light is filtered out. Here we show that to obtain the data necessary for the

Biomedical Optics EXPRESS

calculation of the phasor spectral components we can use in the emission side of the microscope a filter that transmit the light in a "cosine and sine" profile over a bandwidth $\Delta\lambda$. The image obtained when these filters are inserted in the collection path, will directly provide the numerator of the expressions for G and S in Eq. (1) and Eq. (2) after some manipulation as explained below. The denominator could be obtained by removing the filters since the numerator is the total intensity. Using this approach we need to collect 3 images, with the cos and sin filters and without the filters. Then we calculate the G and S coordinates of the spectral phasor at each point of the image using Eq. (1) and Eq. (2). We note that the cos-sin filters are physical components of the microscope. The spectral phasor is obtained at the harmonic n = 1 which depends of the specific transmission of the filters used.

3. Calculation of the cos and sin response of transmission filters

Let us indicate with $F_{cos}(\lambda)$ and $F_{sin}(\lambda)$ the transmission of these two filters and rewrite the G and S coordinates of the spectral phasor in terms of the transmission of the filters. We indicate with $I(\lambda)$ the total intensity measured in the absence of the filters.

Of course, the G and S coordinates obtained from the transmission through the filters are not equal to the mathematical expression of Fourier spectral components given in Eq. (1) and Eq. (2), unless the filters have a perfect cos and sin transmission and they span from −1 to + 1, which cannot be obtained with transmission filters. Therefore, the response of each filter must be shifted and normalized to give the G and S components. Using a spectrophotometer we can easily obtain the transmission of each filter in a given bandwidth $\Delta\lambda$ and in the range between 0 and 1. If we indicate with F_{cosMAX} and F_{cosMIN} the maximum and minimum transmission for the cos filter (and similarly for the sin filter) as determined by the transmission spectrum, we can modify Eq. (1) and Eq. (2) to the following form (only the G component is shown here since the expression for the S component is similar after exchanging the cos with sin). We normalize the filter transmission using the following expression, where $F_{cos}(\lambda)$ is the transmission spectrum of the cos filter at each wavelength (we multiply the transmission by 2 and subtract 1).

$$F(\lambda)_{norm} = 2*(F_{cos}(\lambda) - F_{cos\,MIN}) / (F_{cos\,MAX} - F_{cos\,MIN}) - 1 \quad (3)$$

Now $F(\lambda)_{norm}$ is in the range between + 1 and −1, as it should be for a cosine filter.

The measured normalized total light (I_{cos}) of an unknown spectrum $S(\lambda)$ after passing through the cos filter is given by

$$I_{cos} = (\sum_{\lambda} F_{cos}(\lambda) * I(\lambda)) / \sum_{\lambda} I(\lambda) \quad (4)$$

This total intensity must be normalized using Eq. (3) to give the spectral phasor coordinate G (and similarly for the component S)

$$G = 2(I_{cos} - F_{cos\,MIN}) / (F_{cos\,MAX} - F_{cos\,MIN}) - 1 \quad (5)$$

Note that the normalization procedure only uses the transmission spectrum as obtained with the spectrophotometer of the cosine and sine filters from which the maximum and minimum transmission of the filters is obtained in a given bandwidth $\Delta\lambda$. The normalization factor are measured only once for each filter.

4. Linear combination of the spectral phasor components

The G and S components measured using Eq. (5) have the same properties of the G and S Fourier components in Eq. (1) and Eq. (2). For example, they obey the law of linear combination of components addition as shown below. If I_1 and I_2 represent 2 different spectra and they are mixed in a fractional contribution to the total intensity as f_1 and $f_2 = 1\text{-}f_1$ then we have for each individual spectral component

$$G_1 = \sum_{\lambda} I_1(\lambda) * I_{1cos}(\lambda) / \sum I(\lambda) \quad (6)$$

Biomedical Optics EXPRESS

$$G_2 = \sum_\lambda I_2(\lambda) * I_{1\cos}(\lambda) / \sum I(\lambda) \tag{7}$$

And for the combination of the two components we have

$$G = \frac{\sum_\lambda I(\lambda) * I_{\cos}(\lambda)}{\sum_\lambda I(\lambda)} = \frac{\sum_\lambda f_1 * I_{1\cos}(\lambda)}{\sum_\lambda I(\lambda)} + \frac{\sum_\lambda f_2 * I_{2\cos}(\lambda)}{\sum_\lambda I(\lambda)} = f_1 * G_1 + (1 - f_1) * G_2 \tag{8}$$

There is an analogous expression for the S component. The law of linear combination remains valid provided that $\Sigma_\lambda I(\lambda)$ is the total intensity measured over the entire bandwidth. The same reasoning applies to an arbitrary number of components.

5. Example of cosine and sine filters

We use inexpensive commercial plastic Cyan and Green filters that are sold in large sheets and we cut them to fit the filter holder of the DIVER microscope (Amazon, color filters, cat# B016Q0BA6A approximately $10 for a 18cmx20cm sheet). These filters have a transmission response that is "similar" to a cos-sin response in the spectral region between 400 and 600 nm which is the active wavelength region for the DIVER microscope.

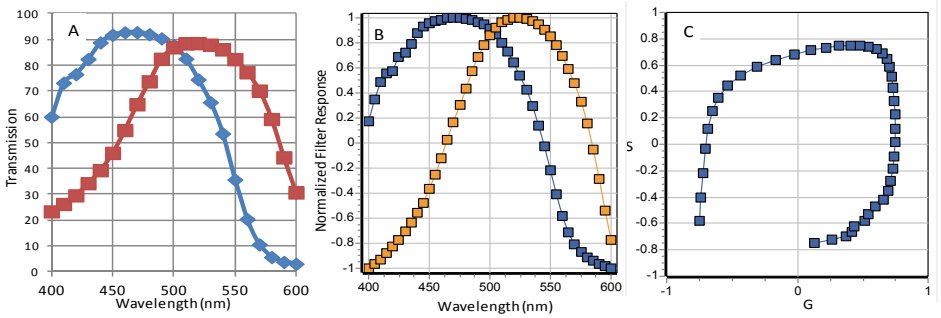

Fig. 1. Cos-sin filters transmission. A) The filters transmission used to obtain the first harmonic of the spectral bandwidth. Outside the region 400nm 600nm the transmission is zero with the addition of bandpass filters. B) The output of the filters is normalized and shifted to give the range of the cosine and sine function. C) The phasor representation of the G and S function obtained with these filters. Note that the polar phasor plot of the filters deviates from the perfect cosine and sine functions (should be a circle).

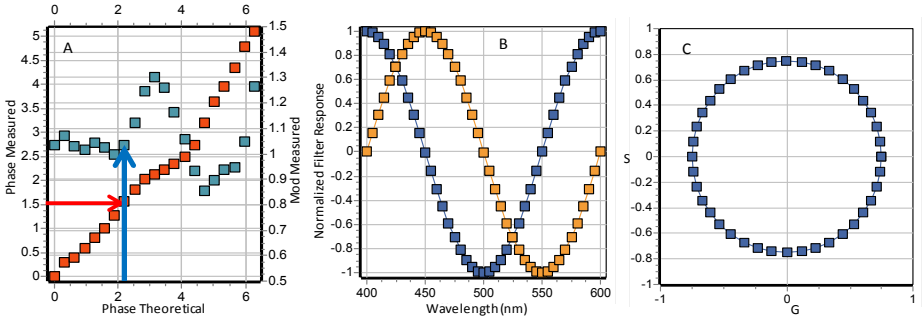

Fig. 2. Correction for the non-ideal response of the filters. A) Correction factors for the phase and amplitude of the filter obtained by comparing the measured response with the ideal response of the cos-sin functions. The phase measured at a given wavelength is compared with the theoretical value (red arrow). For the theoretical value of the phase, the correction factor of the modulation is read from the graph. B) After the correction is applied, the filters have the ideal response. C) The phasor representation of the filter after correction is now a circle, as it should be for a perfect (cos-sin) filter combination.

Biomedical Optics EXPRESS

Figure 1(A) shows the filter transmissions for the cos and sin filters as measured with the spectrophotometer. Figure 1(B) shows the normalized spectrum in the region between 400nm and 600nm. Each of the filter spectrum is first normalized to be between 0 and 2 using the max-min of each spectra transmission and then the normalized spectrum is multiplied by 2 and shifted by −1 so that the value oscillates between + 1 and −1 as it should be for a cosine and sine function. Figure 1(C) shows the phasor polar plot representation according to Eq. (3). Note that the filters in Fig. 1(A) are not exactly representing the cosine and sine functions.

Next in Fig. 2 we calculate the ideal cosine and sine functions for the same spectral region and we plot the deviation of the phase and modulation of the real filters with respect to the ideal filters as shown in Fig. 2(A). The functions in Fig. 2 can be used to "correct" the real filters. Specifically, given a measured phase (red arrow) and the measured modulation as obtained by the real filter, we interpolate the values using the curves of Fig. 2 to obtain the phase and modulation of the ideal filter for each value of the phase. For any given value of the measured phase indicated by the red arrow we obtain the theoretical value of the phase at that point. Then for the theoretical value of the phase we get the correction to the applied to the measured modulation value to obtain the theoretical modulation value at the measured phase. This correction can be done only if the plot of the measured phase with respect to the theoretical phase of Fig. 2 is monotonic. In few words, given a measured phase, we can calculate the corrections for the phase and the corresponding correction for the modulation.

We can use these deviations to correct the filters to obtain the ideal cos-sin shape and then the correspondent phasor plot as shown in Fig. 2(C). However, this correction, albeit small, compromise the law of linear combination because points at different phase are moved to fit the exact position corresponding to the mathematical form of the cos-sin functions. So if the law of linear combination is needed for analysis, we will not use this correction.

6. Behavior of the cos-sin filter in the presence of multiple scattering

To calibrate the cos-sin filter combination in the DIVER microscope, we brought light of different wavelength using a tungsten lump and a monochromator. The output of the monochromator was coupled to the microscope using a mirror. In the DIVER we use collimated light to illuminate the filter with a direction perpendicular to the surface of the filter. This measurement gave us the calibration for a transparent sample. For transparent samples we can obtain the spectral phasor using only the cos-sin filters. Then we added in front of the filters a thick (5 mm) scattering slab as shown in Fig. 3. Also in this case we obtain the spectral phasor with identical resolution as the transparent sample. Our conclusion is that for strongly scattering samples we obtain the same spectral phasor as for the transparent sample.

Biomedical Optics EXPRESS

7. How was the demonstration performed?

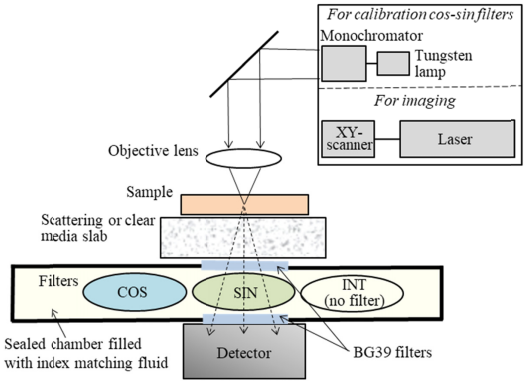

Fig. 3. Experimental setup. The detailed description of the DIVER microscope can be found in [13]. For the demonstration, we show the microscope objective, a container with fluorescence solutions (Sample), a transparent block or scattering block that we insert between the sample and the detector and the position of the Cyan (cos) and Green (sin) filters. The filters were inserted in a rotating filter wheel placed inside the sealed chamber filled with the index matching fluid. Matching refractive index in the optical path from a sample to the detector allows minimizing photon losses due to reflections. For cos-sin filters calibration we used collimated light in the 400-600 nm range, which was generated by passing tungsten lamp light through the monochromator (in this case the objective lens and the sample were removed). For two-photon imaging, the Spectra-Physics InSight DS + femtosecond laser coupled with the scanning system was used as an excitation light source.

The monochromator was moved by increments of 10 nm starting at 400 nm and for each wavelength 3 measurements were acquired, with the cos filter, with the sin filter and without the filters. Each measurement gives one intensity value. The value of I_{cos} was obtained by the ratio of the total intensity through the cos filter to the total intensity without the filter. A similar procedure was used to obtain I_{sin}.

Then Eq. (5) was used to obtain the G and S components of the spectral phasor. The phasor value at the wavelength selected by the monochromator was plotted in the phasor plot. The phase of the phasor spans between 0 to 360 degrees, with zero corresponding to 400nm and 360 degrees corresponding to 600nm. The wavelength corresponding to each angle is shown in Fig. 4. The data collection was repeated with the insertion of the scatter slab in front of the filter. Figure 4 shows the values of the wavelength obtained by this procedure. The correlation between the measured values of the wavelength measured using the spectral phasor follow the expected value. For the collimated light, the correlation is perfect over the entire spectral bandwidth explored. When the scatter material is added in front of the filters, we observe a deviation in the low wavelength range and also a gradual deviation in the long wavelength range, presumably due to scattering. However, the deviation is surprisingly small. The spectral phasor response could be additionally corrected by this small deviation due to scattering. We note that the DIVER response is very low above 600nm due to additional bandpass filters present in the DIVER microscope.

Biomedical Optics EXPRESS

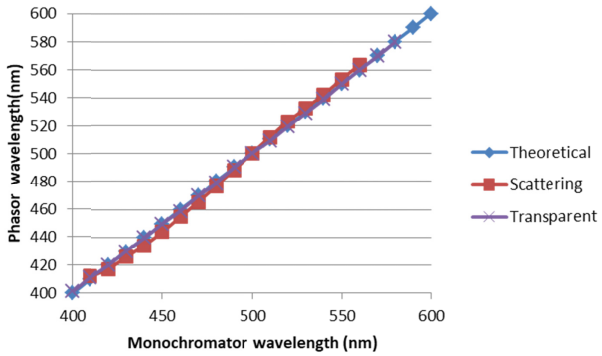

Fig. 4. Calibration of the spectral phasor in the DIVER microscope for a transparent and scattering sample. The expected correlation is perfect for the transparent media and has a very slight deviation due to scattering for the strongly scattering sample.

We have shown that we could use a single channel detector and 3 measurements to obtain the spectral phasor for any sample in a given spectral region. These three measurements can be obtained by rotating a wheel with the two filters and without a filter in rapid succession or projecting the image after passing through the filters in different regions of a camera. This implementation will provide hyperspectral imaging. We note here that the cos-sin filter combination is totally different from the RGB filters used in a color camera. The fundamental difference is that the RGB filters are intended to isolate the response in 3 wavelengths regions while the basic idea of the cos-sin filter is to use the filters to weight the spectral response in different part of the spectrum and then obtain the spectral phasor using the total light transmitted through the filters.

8. Application to solutions of fluorophores

We used the spectral phasor with the DIVER microscope and the sin-cos filters discussed in the previous section with calibration to determine the spectral phasor of 6 different solutions as shown in Fig. 5.

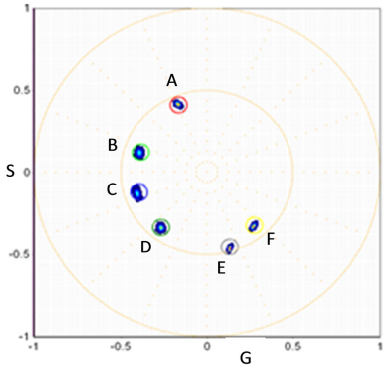

Fig. 5. Measurement of the spectral phasor of 6 dyes. The dyes spectral phasor position recovered using a hyperspectral device (Zeiss LSM 710 with 32 channels spectral detector) and the spectral phasor position recovered by the cos-sin filter method. A) Coumarin 1 /EtOH, 445nm; B) ECFP /buffer, 477nm; C) Coumarin 1/ MeOH, 504nm; D) Rhodamine 110 /water, 520nm; E) Rhodamine 6G/EtOH, 552nm, F) Rhodamine B /water, 576nm.

Biomedical Optics EXPRESS

9. Application of the spectral phasors to strongly scattering samples

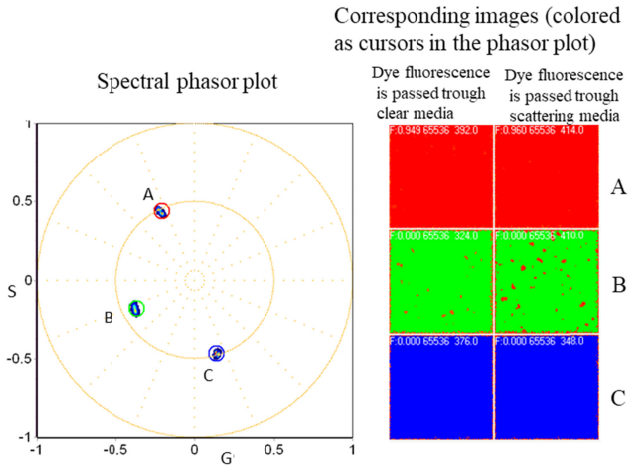

Fig. 6. Spectral phasors of 3 dyes measured with and without the scattering slab. A) Coumarin 1 /EtOH, 445nm; B) Coumarin 1/MeOH, 504nm; C) Rhodamine 6G/EtOH, 552nm. The presence of the scattering slab gives the same spectral phasor as with the transparent slab.

As shown in Fig. 6, each spot has the same spectral phasor with and without passing the light through a clear media of 5mm or a strongly scattering media slab also of 5 mm. The spectral phasor position is not dependent of scattering as shown by the coincidence of the spectral phasor with the clear slab or the scattering slab.

The DIVER microscope due to the efficient light collection acts as an integrating sphere providing the true spectral phasor.

10. Application to demonstrate the law of linear combination of spectral phasors

Although the span and the angular dependence are different for the ideal cos and sin filters and for the actual physical filters, the linear combination law is still valid as demonstrated in Fig. 7.

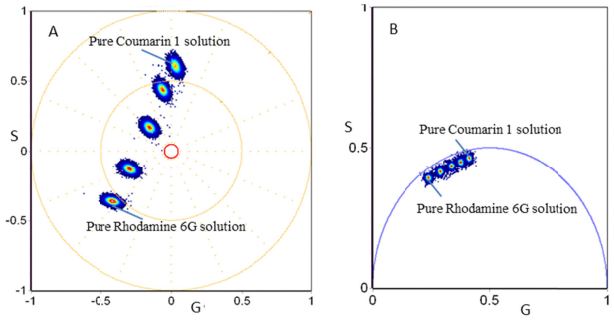

Fig. 7. Linear combination of molecular species. Measurement of spectral phasor for a mixture of Coumarin 1 and Rhodamine 6G ethanol solutions. Concentrations of pure dye solutions were adjusted to yield approximately the same fluorescence signal under two-photon excitation at 740nm. Mixtures containing 0, 25, 50, 75 and 100% of pure dye solution we used for measurements. A) Linear combination of phasor positions obtained using the cos-sin filters and B) linear combination using the lifetime phasor approach. According to phasor linear combination law, phasors of mixed solutions should be positioned on the line connecting phasors of pure solutions. This is demonstrated for both spectral (A) and lifetime (B) phasors measured for dyes mixtures.

Biomedical Optics EXPRESS

In Fig. 7 we show that the law of linear combination is valid for the cos-sin filters provide we don't apply the filter corrections. For comparison, we show the linear combination law obtained using the lifetime phasor for the same solutions used for the spectral phasors.

11. Application to show the spectral phasor of an unknown sample

To compare the performance of the cos-sin filter with hyperspectral images, we use a convallaria slide measured with a commercial hyperspectral method (Zeiss 710 LSM equipped with a 32 channel spectral detector) and using the cos-sin filter. We note that the commercial hyperspectral device covers a wavelength region from 416nm to 726nm, while the cos-sin filter in the DIVER microscope works in the range 400nm to 600nm, therefore spectral difference are expected. However, the purpose of the hyperspectral images of Fig. 8 is to show the similarities between the two images and that the cos-sin filter method is capable of distinguishing pixels with different emission in a slide containing different species emitting at different wavelengths.

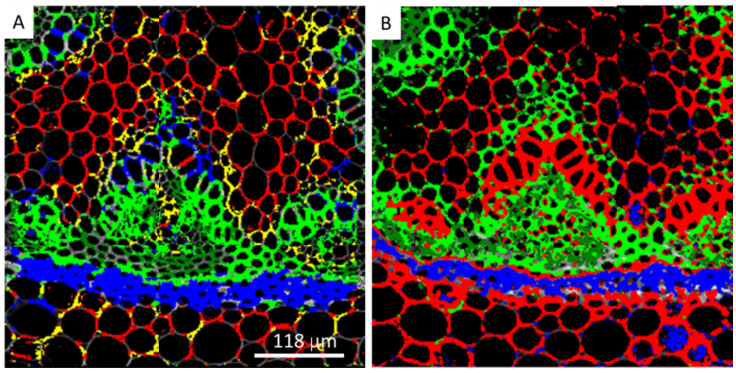

Fig. 8. Comparison of spectral phasor and hyperspectral images of a convallaria sample. A) spectral phasor image obtained with the cos-sin filter in the DIVER microscope. B) Hyperspectral image of the same sample obtained with the wavelength detector of the Zeiss 710 Confocal microscope equipped with the 32-spectral detector. The sample was excited at 740nm using two photon excitation in both cases.

12. Conclusions

Using inexpensive cyan-green filters we can obtain the spectral phasor of solutions and of unknown samples by a simple calibration of the transmission of the filter to the theoretical cosine and sine functions used on the mathematical expressions of the spectral phasor's. We note that there are no adjustable parameters involved in the calibration. The only information needed is the transmission of the filters in the region of sensitivity of the DIVER detector or any other microscope. If new filters are used or the region of sensitivity of the detector is different because the detector has been changed, new correction factors could easily be calculated using the procedure described in this article. The specific filter set used in this work perform the operation of selecting the first harmonic of the spectral bandwidth. If other harmonics are needed, different filters must be installed in the microscope.

Funding

National Institutes of Health (NIH) (NIH P41-GM103540).

Disclosures

The authors declare that there are no conflicts of interest related to this article.